Available online at www.sciencedirect.com
SCIENCE DIRECT®
Polymer 44 (2003) 7821–7827
polymer
www.elsevier.com/locate/polymer

Thermo-sensitive poly(*N*-vinylcaprolactam-*co*-acetoacetoxyethyl methacrylate) microgels: 1—synthesis and characterization

Volodymyr Boyko[a,*], Andrij Pich[b], Yan Lu[b], Sven Richter[a], Karl-Friedrich Arndt[a], Hans-Juergen P. Adler[b]

[a]*Institute of Physical Chemistry and Electrochemistry, Dresden University of Technology, D-01062 Dresden, Germany*
[b]*Institute of Macromolecular Chemistry and Textile Chemistry, Dresden University of Technology, D-01062 Dresden, Germany*

Received 24 March 2003; received in revised form 18 August 2003; accepted 11 September 2003

Abstract

In the present paper, polymeric microgels have been prepared by surfactant-free emulsion co-polymerization of acetoacetoxyethyl methacrylate (AAEM) and *N*-vinylcaprolactam (VCL) in water with water-soluble azo-initiator 2,2′-azobis(2-methylpropioamidine) dihydrochloride (AMPA). It was found that the particle diameter decreased gradually when higher amounts of AAEM were used in monomer mixture. Obtained microgels possess lower critical solution temperature (LCST) in water solutions, so rapid decrease of the particle size was observed at elevated temperatures. As was found using simultaneous static and dynamic light scattering, microgels undergo soft sphere–hard sphere transition during heating.

Keywords: *N*-vinylcaprolactam; Thermosensitive microgel; Functional monomer

1. Introduction

In the recent years, increasing attention has been focused on the preparation and characterization of microgels containing thermosensitive polymers [1–3]. These spherical particles display a strong thermoresponsivity, where below a characteristic lower critical solution temperature (LCST) they are highly swollen in water, but after heating they shrink rapidly to a collapsed polymer globule. The swellability of a microgel depends on the type of microgel, its affinity to the solvent, which in turn is dependent on monomer (and/or comonomer) composition/concentration, as well as degree of cross-linking. The nature of monomer used in preparation of the microgels will determine overall properties of the final product. The addition of the monomers with different functionalities to the microgel can create particles with a wide range of different properties and makes their possible range of application wider.

Poly-*N*-vinylcaprolactam (PVCL) is a thermosensitive polymer, which exhibits LCST at 32 °C [4]. Due to its biocompatibility [5] and complexation ability with different organic compounds [6,7] it is useful in a wide range of applications. Up to now, only a few syntheses of polymers and microgels with different functional groups based on *N*-vinylcaprolactam (VCL) have been reported [8–11].

In this work, we have studied the colloidal and temperature behavior of a novel system based on VCL and hydrophobic comonomer acetoacetoxyethyl methacrylate (AAEM), prepared by precipitation polymerization with cationic initiator in surfactant free conditions. The acetoacetate function of the AAEM can react in a wide range of post modification reactions: reactions with amines, aldehydes, chelation, Michael reaction, etc. [12–14]. Therefore, obtained microgels can be interesting objects for application in medicine or in metal separation.

2. Experimental

2.1. Materials

Acetoacetoxyethyl methacrylate was obtained from Aldrich and purified by conventional methods and then vacuum distilled under nitrogen. VCL was obtained from

* Corresponding author.
E-mail address: volodymyr.boyko@chemie.tu-dresden.de (V. Boyko).

0032-3861/$ - see front matter © 2003 Elsevier Ltd. All rights reserved.
doi:10.1016/j.polymer.2003.09.037

Aldrich and purified by distillation. Initiator, 2,2′-azobis(2-methylpropioamidine) dihydrochloride (AMPA) was obtained from Aldrich and used as received. Deionized water was employed as polymerization medium. Cross-linker *N*,*N*′-methylenebisacrylamide (MBA) from Aldrich was used without further purification.

2.2. Polymerization procedure

Appropriate amounts of AAEM, VCL (see Table 1) and 0.06 g of cross-linker (3 mol%) were added to 145 ml deionized water. A double-wall glass reactor equipped with stirrer and reflux condenser was purged with nitrogen. The solution of the monomers was placed into the reactor and stirred for 1 h at 70 °C with purging with nitrogen. After that the 5 ml water solution of initiator (5 g/l) was added under continuous stirring. Reaction was carried out for 8 h. The polymerization yield, determined gravimetrically, was around 80%. The chemical structure of VCL/AAEM copolymer is presented in Fig. 1. Composition of copolymers in VCL/AAEM microgels was determined by elementary analysis.

2.3. Cleaning procedure

Polymer dispersions were freed from monomers and noncross-linked polymers by dialysis. Latexes were dialyzed against water using Biomax 100 (Millipore) membrane.

2.4. IR spectroscopy

IR spectra were recorded with Mattson Instruments Research Series 1 FTIR spectrometer. Dried samples were mixed with KBr and pressed to form a tablet.

2.5. Thermal analysis

DSC measurements were made with Mettler TA 4000 instrument. TGA measurements were made with TGA 7 Perkin Elmer and Pyris-Software Version 3.51 was used. Before measurement, samples were dried in vacuum for ca 48 h. Samples were analyzed in closed aluminum cups. Measurements were made at heating rate 5 °C/min in nitrogen atmosphere.

Table 1
Reaction recipe for preparation of AAEM/VCL microgels

Run	VCL (g)	AAEM (g)	AAEM (mol%)[a]
1	2.06	0.04	1.25
2	2.04	0.08	2.5
3	1.98	0.16	5
4	1.93	0.24	7.5
5	1.88	0.32	10

[a] Predicted value.

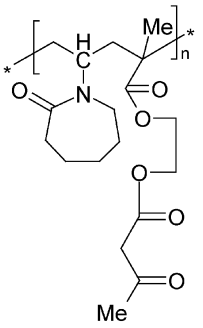

Fig. 1. Chemical structure of VCL/AAEM copolymer.

2.6. Particle size analysis

A commercial laser light scattering (LLS) spectrometer (ALV/DLS/SLS-5000) equipped with an ALV-5000/EPP multiple digital time correlator and laser goniometer system ALV/CGS-8F S/N 025 was used with a helium–neon laser (Uniphase 1145P, output power of 22 mW and wavelength of 632.8 nm) as the light source.

With static LLS it is possible to obtain both the weight-average molar mass (M_w) and the *z*-average radius of gyration R_g of scattering objects in an extremely dilute solution because Rayleigh ratio $R(q)$, is dependent on the scattering vector q as:

$$\frac{Kc}{R(q)} = \frac{1}{M_w}\left(1 + \frac{(qR_g)^2}{3}\right) + 2A_2c \tag{1}$$

where

$$K = 4\pi^2 n^2 (\mathrm{d}n/\mathrm{d}c)^2/(N_A\lambda_0^4) \tag{2}$$

$$q = (4\pi n/\lambda_0)\sin(\theta/2) \tag{3}$$

with n, N_A, λ_0, θ being the solvent refractive index, the Avogadro's number, the wavelength of the incident light in a vacuum, the scattering angle and concentration, respectively.

In dynamic LLS, the intensity–intensity–time correlation function $g_2(q,t)$ in the self-beating mode was measured and can be expressed by the Siegert relation:

$$g_2(q,t) = A(1 + \beta|g_1(q,t)|^2) \tag{4}$$

where t is the decay time, A is a measured baseline, β is the coherence factor, and $g_1(q,t)$ is the normalized first-order electric field time correlation function and $g_1(q,t)$ is related to the measured relaxation rate Γ:

$$g_1(q,t) = \exp(-\Gamma t) = \int G(\Gamma)\exp(-\Gamma t)\mathrm{d}\Gamma \tag{5}$$

A line-width distribution $G(\Gamma)$ can be obtained from the Laplace inversion of $g_1(t)$ (CONTIN procedure). For a pure diffusive relaxation, Γ is related to the translational diffusion coefficient D at $q \to 0$ and $c \to 0$ by

$$D = \Gamma/q^2 \tag{6}$$

or a hydrodynamic radius R_h given by

$$R_h = k_B T/(6\pi\eta D) \quad (7)$$

with q, k_B, T and η being scattering vector, the Boltzman constant, absolute temperature, and solvent viscosity, respectively. All DLS experiments were carried out at angles $\theta = 30-140°$. The concentration of the microgel in water was about 1.5×10^{-5} g/ml. Microgel solutions were filtrated using 5 μm nylon filters. Typically, the sample in a 10 mm test tube was immersed in a toluene bath and thermostated within an error of ±0.1 °C.

Typically, three measurements were performed for determination of the radius of gyration and five for the hydrodynamic radius. Accuracy of measurements for radius of gyration is ±6%, for hydrodynamic radius is ±3%.

2.7. Stability measurements

Stability measurements were performed with separation analyser LUMiFuge 114 (L.U.M. GmbH, Germany). Measurements were made in glass cuvettes at acceleration velocity 3000 rpm. The slope of sedimentation curves was used to compare the stability of the samples.

2.8. Scanning electron microscopy (SEM)

Scanning electron images were taken with Gemini microscope (Zeiss, Germany). Dispersions were diluted with deionized water, dropped onto aluminum support and freeze dried. Pictures were taken at voltage of 4 kV.

3. Results and discussion

3.1. Synthesis of VCL/AAEM microgels

The amounts of reagents used for preparation of AAEM/VCL microgels are summarized in Table 1.

In all cases stable milky dispersions were obtained. Incorporation of AAEM in microgel was checked with IR spectroscopy. Typical IR spectrum for copolymer microgel is showed in Fig. 2. Major changes can be observed in region 1500–1800 cm^{-1}. Characteristic signals for PVCL (amide at 1623 cm^{-1}) [15] and for PAAEM (C=O at 1745 cm^{-1}) are marked with arrows. It should be noted, that signal for PAAEM consists of vibration of both ester and ketone carbonyls, which cannot be completely discriminated in this case.

It is well known [16], that copolymerisation of *N*-vinyl monomers with methacrylic ones is not ideal due to large difference in reactivity. Besides, faster consumption of acrylic cross-linker leads to formation of some non-crosslinked polymers based mostly on the PVCL. So, incorporated amounts of AAEM presented in microgels are higher than it is taken in starting monomer mixture (see Fig. 3). It should be noted, that elementary analysis is not exact

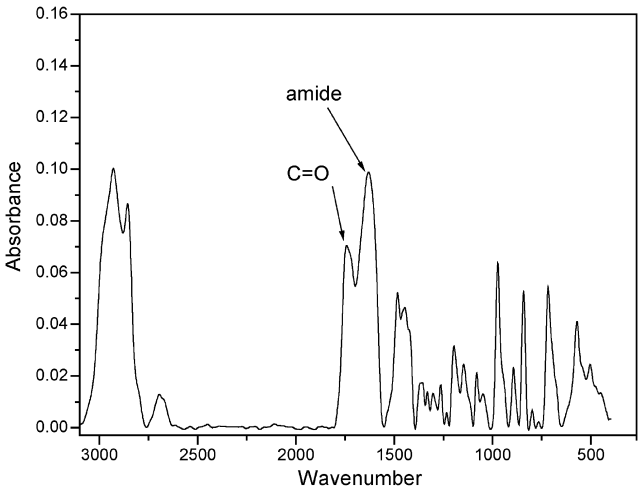

Fig. 2. IR spectra of VCL/AAEM copolymer microgel (run 4).

method for determination of composition of polymers based on *N*-vinyl lactams [17], so AAEM content in microgels determined by elementary analysis does not correspond to the real amount of AAEM in copolymer structure.

Incorporation of AAEM units ($T_g^{PAAEM} = 18$ °C [12]) in copolymer leads to decrease of glass transition temperature of network to 60–80 °C ($T_g^{PVCL} = 147$ °C [18]). No clear dependency of T_g on co-polymer composition was observed. This fact can be explained by the presence of bounded water, which cannot be easily removed and strongly influences glass transition of PVCL [18]. TGA measurements indicate that VCL/AAEM copolymers are thermally stable in nitrogen atmosphere up to 300 °C.

3.2. Stability and particles size

The sedimentation of VCL/AAEM dispersions was investigated by method developed by Lerche et al. [19]. In special centrifuge an integrated optoelectronic sensor system allows spatial and temporal changes of light

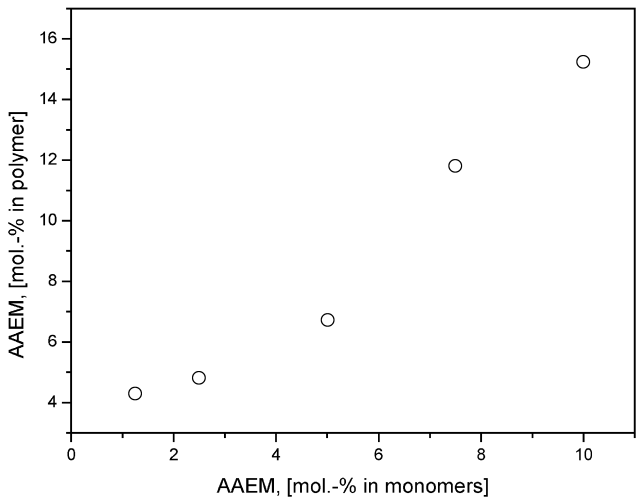

Fig. 3. Incorporation amount of AAEM in microgel as function of AAEM content in monomer mixture.

transmission during the rotation to be detected. In contrast to other approaches [20] the local transmission is determined over the entire sample length simultaneously. Throughout the measurement, transmission profiles are recorded and sedimentation process can be depicted as a time course of the relative position of the boundary between supernatant and sediment (resolution better than 100 μm) or of the transmission averaged over the entire or a chosen part of the sample length. On the basis of the obtained data the sedimentation constants, the packing density, etc. can be derived [19].

The transmission profile of sedimentation process for sample 5 in Fig. 4a shows continuous decrease in sediment height due to compression of the sediment. In this case the transmission profiles were recorded every 10 s and every 100th measurement is shown. Fig. 4a shows that a sedimentation fronts move parallel to the cuvettes bottom. The transmission profiles can be transformed into transmission-time curves (Fig. 4b). The transmission increases with centrifugation time since particles move to the bottom of the cell. Fig. 4b presents transmission-time curves for VCL/AAEM particles prepared at different compositions. The slope of the sedimentation curves indicates that particles, which contain high AAEM amounts, precipitate faster if to compare with particles containing less AAEM.

The calculated sedimentation rates from the slopes of transmission-time curves are summarized in Fig. 5. The sedimentation rate increases nearly in linear order with increasing AAEM content in particle structure. The values of average hydrodynamic radius measured by DLS for different microgels decrease gradually with increasing AAEM content. The sedimentation rate (ν) for particles in diluted system can be defined as:

$$\nu = \frac{2r^2 \Delta\rho x g}{9\eta} \tag{8}$$

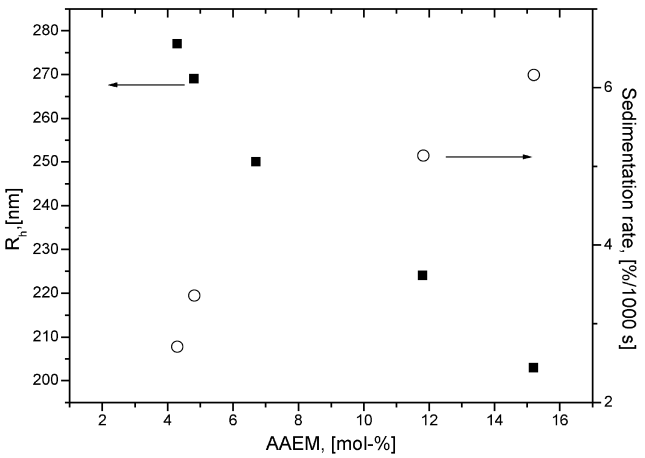

Fig. 5. Hydrodynamic radius of microgels (solid symbols) and sedimentation rate (open symbols) as a function of AAEM content ($T = 20$ °C).

where r is particle radius; $\Delta\rho$ is density difference; xg is centrifugal force; and η is the viscosity of medium. Since the viscosity of the medium and centrifugal force ($xg = 1200$ [1/9,81 m/s^2] for cuvette radius 12 mm and rotation speed 3000 rpm) are constant for all microgels, the sedimentation velocity can be influenced by particle size or density difference between particles and medium. The analysis of Eq. (8) with respect to the experimental data presented in Fig. 5 leads to conclusion that increase of sedimentation rate which is accompanied by decrease of the particle radius must result in increase of $\Delta\rho$ values due to the incorporation of AAEM units. It is supposed, that AAEM induces some additional cross-linking in the microgel particles by the chain transfer reaction on methylene group of diketone functionality [21] and thus increases particle heterogeneity. In other words, more dense internal structure should be formed at higher concentrations of AAEM.

It should be noted, that AAEM improves the stability of

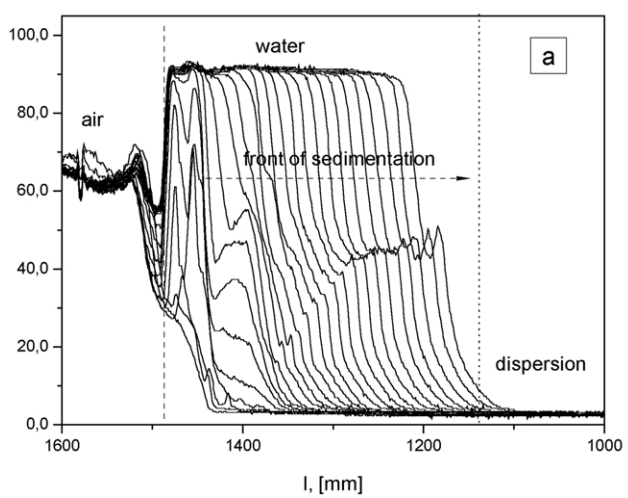

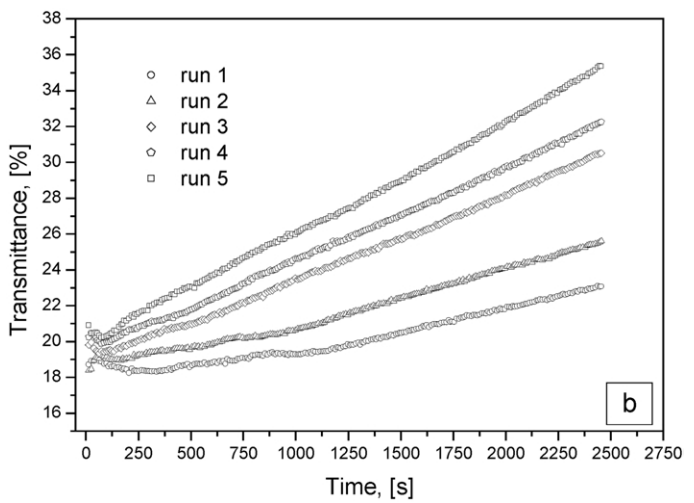

Fig. 4. Front of sedimentation (a) of the microgel (15.2 mol% AAEM) and sedimentation curves (b) for different microgels.

VCL chains in water, and when no AAEM is used in reaction recipe, the particles coagulate during polymerization process. Also, VCL/AAEM particles are quite stable and can be very slowly sediment at high centrifugation rates (determined sedimentation rates are low). From this point of view, AAEM cannot be treated like component, which reduces the stability of the whole particles. The stability of the VCL/AAEM particles toward electrolytes was also investigated. Addition of electrolyte (NaCl) to dispersions to some extent does not influence stability. High concentration (1 M solution) makes dispersions unstable due to shift of LCST of PVCL to lower temperatures. Collapse of VCL fragments leads to absence of the sterical stabilization and additional screening of charged initiator fragments induces coagulation of particles.

3.3. Thermosensitive properties

The particle size of VCL/AAEM microgels was measured at different temperatures. Fig. 6 represents temperature dependencies of microgels size. It is surprising, but there are no differences in the transition temperature (Fig. 6a) between particles with different content of hydrophobic AAEM. For all samples the broad continuous decrease of hydrodynamic radius was detected, and transition temperature was slightly shifted to ~28 °C in comparison to reported 32 °C for PVCL [4]. It is also seen, that all microgels shrink to approximately the same size, although difference in swelling is significant. The behavior of radius of gyration (R_g) is similar to that of R_h, but at temperatures above LCST R_g values are higher for samples with lower AAEM content.

It is also clear from the R_g values presented in Fig. 6b, that increasing of AAEM concentration increases hydrophobicity of the core and makes the core more dense and compact. This leads to the decreasing of the thermosensitivity of the core and transition temperature shifted to 23–24 °C.

The particles size distributions for the sample 5 (15.2 mol% AAEM) at different temperatures are shown in Fig. 7.

Heating of the microgel dispersion does not influence polydispersity of particles size distribution. Note, that Laplace inversion requires some smoothing of the experimental data and this may cause a broader distribution than actually present [22].

It is well known that the ratio $\rho = R_g/R_h$ reflects the conformation of a polymer chain or the density distribution of a particle and thus gives valuable information about the internal structure of microgels. Fig. 8 shows the ρ parameter as function of the temperature calculated from experimental R_g and R_h data presented in Fig. 6.

It is useful to consider this ratio because the influence of molar mass dependencies can be neglected [23]. The typical ρ values for microgels in range 0.3–0.6 have been reported [24,25]. Theoretically predicted ρ value for the homogeneous sphere is 0.775 and some experimental results confirm this value [26]. Monitoring of ρ parameter shows that with increasing of temperature mobility of PVCL chains decreases and a compact structure without internal motion is formed. As result, microgel exhibits hard sphere behavior (deviations from theoretical value are within experimental error). Up to now only a few observations of the transition from soft to hard sphere have been reported for the microgels, based on thermosensitive polymer [27].

It is worth mentioning the polymerization mechanism in present system to summarize the experimental results presented above. Microgel particle formation occurs by homogenous nucleation that is known sometimes to give latex dispersions with a narrow particle size distribution [28]. At the first stage, a water-soluble cationic radical initiates mainly a water-soluble (in present concentrations)

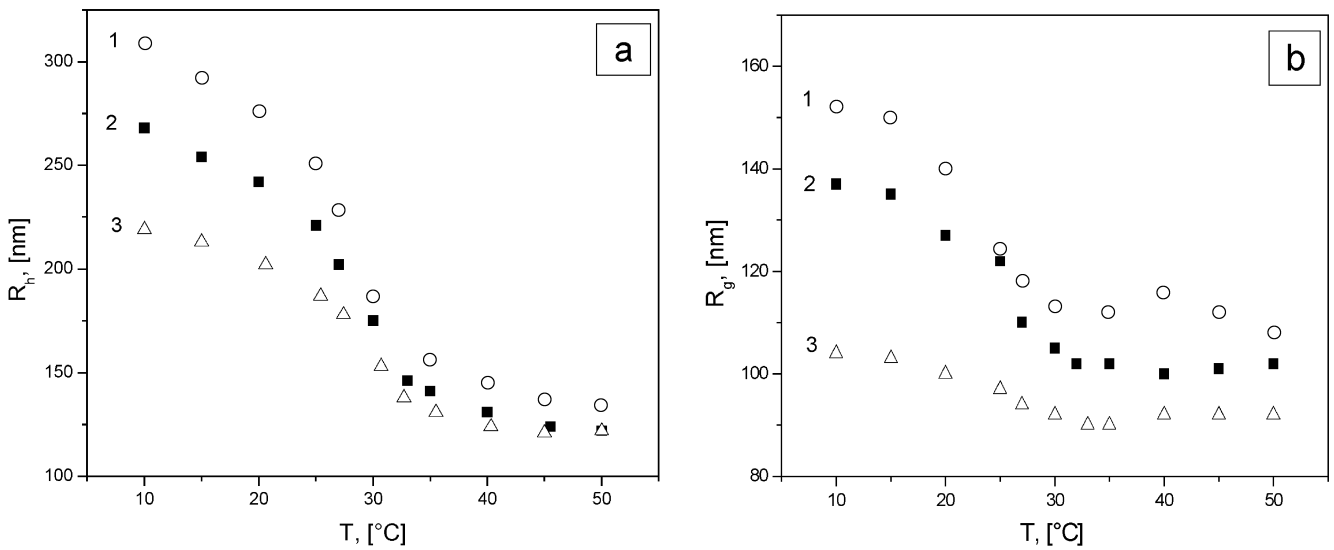

Fig. 6. Average hydrodynamic radius (a) and radius of gyration (b) as a function of the temperature; 1—run 1, 2—run 3, 3—run 5.

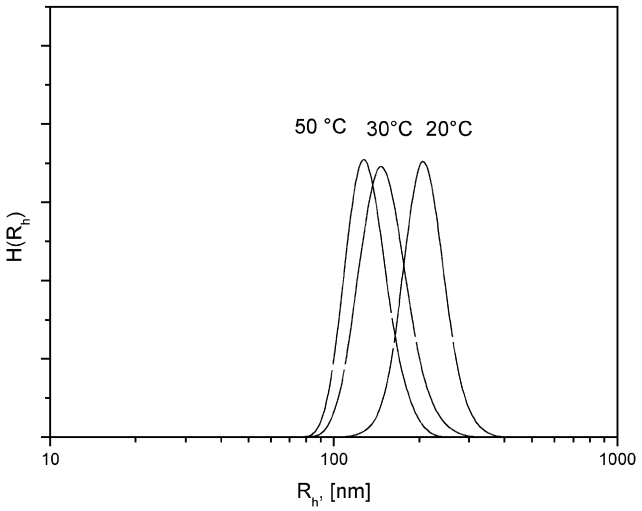

Fig. 7. Hydrodynamic radius distribution (run 5; 15.2 mol% AAEM) as a function of the temperature at the observation angle $\theta = 90°$.

AAEM and MBA monomers which then grows in solution until they reach a critical chain length after which the growing chain precipitates to become a colloidally unstable 'precursor particle'. The precursor particles follow one of two competing processes. Either they deposit onto an existing colloidally stable polymer particle or they aggregate with other precursor particles until they form a particle sufficiently large to be colloidally stable. These stable particles create nuclei for PVCL growing chains. Particle grow occurs up to consumption of the pedant double bounds, which should be available on the particle/water interface due to more hydrophilic character of MBA [1], and further reaction leads only to physical anchoring of the hydrophobic chains. At the polymerization temperature of 70 °C which is far above the LCST, the growing PVCL microgel particles are colloidally stabilized by electrostatic stabilization originating from charged groups introduced by the cationic initiator. It can be supposed that resulting

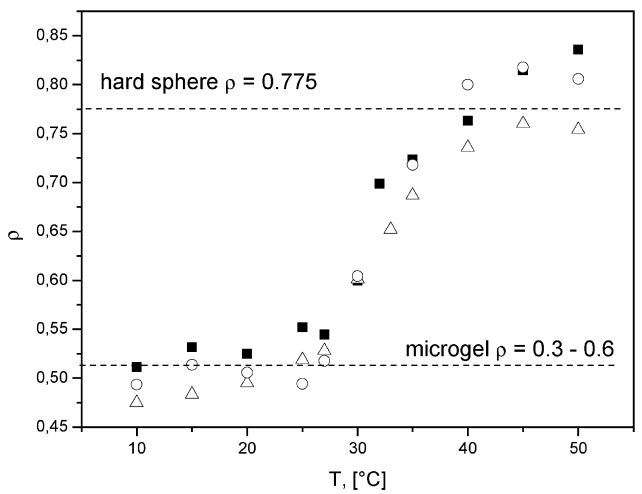

Fig. 8. Temperature dependence of ρ ratio of the VCL/AAEM microgels; circles—run 1, quadrates—run 3, triangles—run 5.

particles have a core-shell structure due to fast consumption of high reactive AAEM on the first stage of reaction. Only in this case the absence of influence of the hydrophobic monomer on the thermal behavior of copolymeric microgel can be expected. Similar structure was observed for copolymer microgels of NIPAM with hydrophobic vinyl laurate [29]. The shell consists mainly of covalently bonded PVCL chains, which in swollen state at low temperatures sterically stabilize microgels. As result, concentration of AAEM only slight influences size of formed particles but regulates degree of swelling and thus size at the temperature below LCST (Fig. 5).

Scanning electron microscopy images for sample with 4.8 mol% AAEM are shown in Fig. 9. It is difficult to obtain good pictures for microgels with this method due, probably, to a strong influence of water on glass-transition of polymer chains. This influence cannot be avoided even with freeze-drying [30].

In general, freeze-drying did little damage and some types of microgels were more susceptible than others. It is also found, that positively charged particles have tendency to form aggregates during drying [31]. In any case, it is possible to recognize individual particles relatively uniform in size.

4. Conclusions

Thermosensitive microgels based on VCL and AAEM have been prepared in surfactant free conditions. Incorporation of hydrophobic comonomer influences stability of obtained particles. Overall VCL: AAEM ratio determines size of microgels below LCST due to regulation of cross-linking (swelling), but only slightly influences size of collapsed particles. The microgels have core–shell structure due to fast consumption of more reactive methacrylic monomer. Transition temperature of the PVCL-rich shell is shifted to ~28 °C in comparison to reported 32 °C for pure PVCL. AAEM-rich particle core is more hydrophobic and is less temperature sensitive if to compare with VCL-rich shell. VCL/AAEM microgel particles exhibit soft sphere-hard sphere transition induced by collapse of highly swollen VCL-rich shell during heating.

Acknowledgements

The authors are thankful to Mrs E. Kern for SEM measurements; Mrs M. Dziewiencki for IR-spectroscopy measurements; Deutsche Forschungsgemeinschaft (DFG, Sonderforschungbereich 287 'Reactive Polymers') and the European Graduate School 'Advanced Polymer Materials' (EGK 720-1, DFG) for financial support. Dr S. Richter thanks the Deutsche Forschungsgemeinschaft (DFG) for financial support (grant-no. RI 1079/1-2).

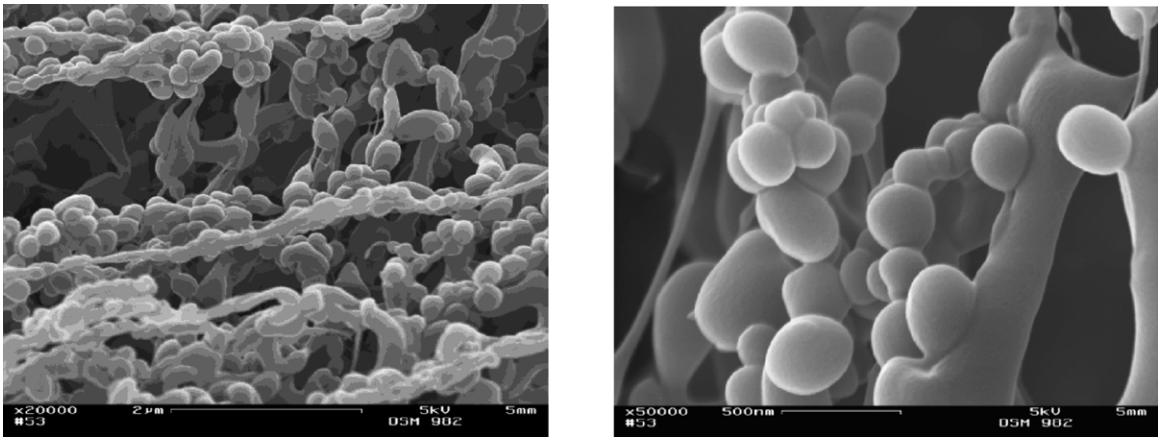

Fig. 9. SEM images of VCL/AAEM microgels.

References

[1] Pelton R. Adv Colloid Interface Sci 2000;85:1.
[2] Duracher D, Elaïssari A, Pichot C. Colloid Polym Sci 1999;277:905.
[3] Hu Z, Lu X, Gao J, Wang C. Adv Mater 2000;12:1173.
[4] Gao Y, Au-Yeung SCF, Wu C. Macromolecules 1999;32:3674.
[5] Vihola H, Laukkanen A, Hirvonen J, Tenhu H. Eur J Pharm Sci 2002; 16:69.
[6] Qui Q, Somasudaran P, Pethica BA. Langmuir 2002;18:3482.
[7] Anufrieva EV, Gromova RA, Yu KE, Yanul NA, Krakovyak MG, Lushchik VB, Pautov YD, Sheveleva TV. Eur Polym J 2001;37:323.
[8] Peng Sh, Wu C. Macromolecules 2001;34:568.
[9] Ivanov AE, Kazakov SV, Iyu G, Mattiason B. Polymer 2001;42:3373.
[10] Makhaeva EE, Tenhu H, Khohlov AR. Macromolecules 2002;35: 1870.
[11] Laukkanen A, Hietala S, Maunu SL, Tenhu H. Macromolecules 2000; 33:8703.
[12] Eastman Chemical Company 1999; N-319 C.
[13] Argaval R, Bell JP. Polym Engng Sci 1998;38:299.
[14] Bertolin M, Zecca M, Favero G, Palma G, Lora S, Ajo D, Corain B. J Appl Polym Sci 1997;65:2201.
[15] Maeda Y, Nakamura T, Ikeda I. Macromolecules 2002;35:217.
[16] Faragalla MM, Hill DJT, Whittaker AK. Polym Bull 2002;47:421.
[17] Peppas NA, Gehr TWB. J Appl Polym Sci 1979;24:2159.
[18] Yu KE, Yanul NA, Kalninsh KK. Eur Polym J 1999;37:305.
[19] Sobisch T, Lerche D. Coll Polym Sci 2000;278:369.
[20] Killmann E, Eisenlauer J. Prog Colloid Polym Sci 1976;60:147.
[21] Hoeshele GK, Andelman JB, Gregor HP. J Phys Chem 1958;62(10): 1239.
[22] Stauch O, Schubert R, Savin G, Burchard W. Biomacromolecules 2002;3:565.
[23] Burchard W. Adv Polym Sci 1999;143:115.
[24] Burchard W. Adv Polym Sci 1983;48:1.
[25] Burchard W, Shmidt M, Nerger D. Polymer 1979;20:528.
[26] Pich A, Lu Y, Adler H-J. Coll Polym Sci 2002; published on www.
[27] Senff H, Richtering W. Coll Polym Sci 2000;278:830–40.
[28] Gilbert RG. Emulsion polymerization: a mechanistic approach. London: Academic Press; 1995.
[29] Benee LS, Snowden MJ, Chowdhry BZ. Langmuir 2000;18:6025.
[30] Agbugba CB, Hendriksen BA, Chowdhry BZ, Snowden MJ. Colloids Surf A 1998;137:155.
[31] Zimehl R, Lagaly G, Mielke M, XX Hamburger Makromolekulares Symposium, 22–23 September; 1997.